Comparison of Satellite, Ground-Based, and Modeling Techniques for Analyzing the Urban Heat Island

James A. Henry
Department of Geography, University of Florida, Gainesville, FL 32611
Steven E. Dicks
Southwest Florida Water Management District, Brooksville, FL 34609-6899
Orjan F. Wetterqvist
Department of Urban/Regional Planning, University of Florida, Gainesville, FL 32611
Stephen J. Roguski
Department of Geography, University of Florida, Gainesville, FL 32611

ABSTRACT: The main techniques used to measure and predict urban heat islands have been station comparisons, auto traverses, remote sensing, and modeling. Very few studies have compared the results from using several of these techniques for the same city. This study compares six temperature patterns obtained from the Heat Capacity Mapping Mission satellite with a temperature pattern acquired using the auto-traverse technique and a thermal pattern predicted by a land-use based simulation model called DYNASPACE for a portion of Alachua County, Florida, centered on the city of Gainesville.

The satellite data reveal daytime heat islands of 5 to 6° C and early morning magnitudes of up to 9° C. Highest temperatures during days and mornings were in the central business district (CBD), the university campus, and the airport. Other consistent thermal features in the satellite data were extensions of high temperatures to the north and east of the CBD, and a stronger temperature gradient to the west of the CBD than to the east. All of these features were also apparent in the auto-traverse temperature pattern and were generally predicted by the DYNASPACE model.

INTRODUCTION

MANY STUDIES OF URBAN THERMAL PATTERNS have appeared over the past four decades. The main techniques employed to measure and predict urban heat excess compared with the surrounding rural environment (the urban heat island) have been urban-rural meteorological station comparisons, the auto-traverse method, remote sensing – particularly using aircraft and satellite thermal infrared data, and computer modeling approaches. Each technique measures or analyzes a different aspect of urban-rural temperature differences, and there are caveats associated with each. The urban-rural-station-comparison approach is plagued with the problem of whether the chosen stations are representative of general urban and rural conditions or are indicative of only the immediate local environment. Additionally, no urban heat island spatial distributions can be produced by the two-station method. Studies employing many measuring points represent an improvement of the method, as shown by Hsu's (1984) map of temperatures in and around Phoenix, which was based on 26 recording stations in the Salt River Valley, Arizona. However, the problem of station representativeness remains.

The auto-traverse method, unlike the station-comparison technique, has facilitated the understanding of the spatial variability of urban heat islands. However, persistent problems with this technique include (1) the auto is confined to roads; (2) the traverses, especially if they are circuitous through many parts of the city, may take several hours, sometimes requiring time-standardization techniques applied to the data; and (3) all measurements are acquired at subroof level, which may not necessarily be representative of the surface where the most important energy exchanges occur. The third problem above is discussed in detail by Arnfield (1982), especially in terms of radiation exchanges.

A relatively recent alternative measuring scheme for determining urban heat islands includes obtaining measurements from remote sensing data. Many aircraft-based studies have appeared in the literature. Two general shortcomings of this technique have been that very few data collection periods were involved in each study, and strips of portions of the cities were obtained, rather than entire cities and the surrounding countryside.

Urban heat islands have also been studied using remotely sensed data acquired from satellites. These data overcome many of the problems of the other techniques, and several researchers have suggested these type of data are the most viable for urban heat island studies because they allow averages taken over different portions of the city to be used, are more representative of the urban canopy as a whole, and provide the capability of repeated, synoptic coverage. Rao (1972) presented an urban heat island image obtained by the ITOS-1 satellite for 19 October 1970. Several studies of urban heat islands using various satellite sensors have appeared since this early study of Rao (e.g., Carlson *et al.*, 1977, 1981; Matson *et al.*, 1978; Price, 1979; Winiger, 1982; Kalma *et al.*, 1983; Vukovich, 1983).

Computer simulation models have also been used to study the effects of urbanized areas on the thermal structure of the atmosphere. Terjung (1976) and Oke (1982) point out the advantages of this process-response approach, that allows the prediction of the space-time variations of the morphological components of the atmosphere, interfaces, and substrates. Some urban climate modeling efforts include Outcalt (1972), Terjung and Louie (1973, 1974), Tuller (1975), Pease *et al.* (1976), Morgan *et al.* (1977), Brazel and Johnson (1980), Nunez and Oke (1980), Terjung and O'Rourke (1980), Goward (1981) Arnfield (1982), and Burt *et al.* (1982). Rayner (1984) discusses contributions to urban modeling and general climatological modeling. Todhunter (1986) presents a very detailed analysis of computer simulations of urban effects on the atmosphere. One problem encountered in most modeling simulations is that of parame-

PHOTOGRAMMETRIC ENGINEERING AND REMOTE SENSING,
Vol. 55, No. 1, January 1989, pp. 69–76.

0099-1112/89/5501–69$02.25/0

terizations, which are simplified approximations of actual conditions; these are usually required because of computer limitations and/or lack of data in regard to certain aspects of the modeling process. As noted by Rayner (1984), although parameterizations will be required in most models, considerable effort is being applied toward this particular problem.

Each of these techniques for studying the urban heat island has its own strengths and weaknesses and analyzes a different aspect of the radiative/thermal environment of urban areas. Very few studies compare and contrast results obtained from these diverse techniques. The primary purpose of this study is to assess the correspondence of satellite-derived temperature patterns with a temperature pattern obtained using the auto-traverse technique and a thermal pattern predicted by a land-use-based energy balance model—DYNASPACE—for the city of Gainesville, Florida (population 84,900 at the time of satellite data collection). This will produce, to the authors' knowledge, the only study of an urban heat island for a city using modeling, satellite, and ground-based techniques. There are two secondary aspects that are outgrowths of the primary purpose: (1) general aspects of the urban heat island magnitude and variability in Gainesville are briefly discussed, and (2) the utility of satellite thermal infrared data with a spatial resolution of 600 m for determining intraurban temperature patterns is shown.

SATELLITE AND LAND-USE DATA AND METHODOLOGY

The satellite data used in this analysis are from the Heat Capacity Mapping Mission (HCMM) satellite system. This satellite had a near-polar orbit at an altitude of 620 km and was in operation from April 1978 to September 1980. Visible (0.5 to 1.1 micrometres) and thermal infrared (10.5 to 12.5 micrometres) data are available for approximately 1330 and 0230 LST for northern middle latitudes. These times were chosen because they are most favorable for the determination of surface thermal properties, exchanges of surface heat and moisture with the atmosphere, and the surface energy budget. The resolution of 600 m at nadir of the thermal channel (with the data processed to a pixel size of 481.5 m) has been shown to reveal basic characteristics of urban heat islands (Price, 1979).

The HCMM satellite data were chosen over those available from other satellites for several reasons. The 600-m resolution is significantly better than that available from the currently active Advanced Very High Resolution Radiometer (1.1 km) onboard various NOAA satellites. Also, although the thermal infrared channel of Landsat has a better spatial resolution than HCMM, the overpass times of Landsat (late morning and early evening) are not as conducive as the overpass times of HCMM for urban heat island studies (Price, 1984, 1986). The dates of the HCMM data analyzed here, and shown in Table 1, represent cloud-free data covering three seasons. No cloud-free data for summer were available.

TABLE 1. HEAT CAPACITY MAPPING MISSION SATELLITE THERMAL INFRARED DATA AND METEOROLOGICAL CONDITIONS

Date/Time	Wind	Cloud Cover
Afternoon (1330 LST)		
28 March 1979	Calm	Clear*
5 November 1978	Calm	Clear
17 December 1978	2.0 m/sec, WNW	Clear
Morning (0230 LST)		
1 February 1979	4.0 m/sec, WNW	Clear
21 May 1978	Calm	Clear
3 November 1978	3.1 m/sec, NNE	Clear

* Except for two small cumulus clouds (cool temperatures in Figure 2) at southeast corner of Newnan's Lake, directly east of the city

Five basic procedures were applied to the HCMM thermal infrared data: (1) correction for radiative absorption and emission by atmospheric water vapor; (2) conversion of the digital numbers to temperatures, including correction of HCMM radiometer calibration problems; (3) geometric correction; (4) production of computer-generated isotherm maps using the SURFACE II graphics program; and (5) generation of overlayed isotherm-land use/cover maps.

HCMM DATA PROCESSING

Correction for atmospheric water vapor absorption and emission was applied to obtain actual urban-rural temperatures, rather than relative temperature differences only. The radiative transfer model of Price (1983, and personal communication) was employed. The model requires the input of emissivity and vertical atmospheric sounding data – pressure, temperature, and dew point – determined by a radiosonde. For emissivity, a spatially constant surface value of 0.97 was used, the choice of which was based on several factors. Taylor (1979) in a study of emissivities for soils in southeast United States, showed for the Gainesville, Florida area a value of 0.97 in the 10.4 to 12.6 micrometre portion of the spectrum. Grasslands in the same area have a value of 0.98 to 0.99. Vegetation with an open canopy has an emissivity of 0.96, while closed canopy vegetation values are 0.97 to 0.98. Urban surfaces generally exhibit a wider range of values, but tar/stone, common roofing materials in Gainesville, have a value of 0.97. Artis and Carnahan (1982) noted that most roofing materials are confined to a very narrow range of emissivities and that the variation in rooftop emissivities has a minimal effect on temperatures. In relation to the atmospheric sounding data required, the closest non-coastal radiosonde station to Gainesville, Florida is Waycross, Georgia, 180 km north of the study area. Waycross radiosonde data collected closest to the HCMM overpass times were used. Price noted that surface temperatures within plus or minus 2 to 3° C of actual temperatures are obtainable with this method. Temperatures (°C) were derived from these atmospherically-corrected data using the appropriate equation (National Aeronautics and Space Administration, 1980); known HCMM radiometer calibration errors were discussed by Barnes and Price (1980) and were accounted for here using information from Vukovich (1984).

Geometric correction of the six satellite digital image data sets was obtained by registering one data set to UTM coordinates and digitally overlaying the remaining five images to the registered image. Fifty-one ground control points were used to obtain the UTM registration. A linear mapping function and bilinear interpolation resampling produced a registration with 0.58 pixel error. This accuracy compares favorably to several other recent HCMM studies, where errors of one pixel up to five pixels have been noted.

LAND COVER ANALYSIS

The distribution of land uses/covers was initially obtained from a 1974 map of the county in which the study area occurs. There were two problems with this map: it was based on 1974 data, rather than 1978-79, which are the years of the HCMM data, and it contained 20 classes, which was considered too many for use with this study. The first problem, that of updating the map, was resolved using two data sources. The city of Gainesville had produced a 1978 land-use/land-cover map for the area within the city limits. That portion of the study area outside the city limits was updated using 1979 aerial photography. Relatively few major changes occurred in the study area between 1974 and 1978-79. The second problem, that of too many land-use/land-cover classes, was initially attempted to be solved by combining classes to fit within those presented by Arnfield (1982), which were developed for Columbus, Ohio. However, four of the eight classes (COM2-COM5) do not occur in Gainesville, and the classification does not include rural land covers (Arnfield developed it specifically for use with radiation properties and budgets in cities). The land-use/land-cover scheme of Auer (1978) developed for St. Louis was also considered, which included what he called a "meteorologically significant" land use mosaic. Again, several of the categories do not apply to Gainesville and its surroundings. The classification scheme that produced the best results was the well-known Anderson classification (Anderson *et al.*, 1976), developed especially for aerial photography and satellite data. The use of this system produced the eleven classes shown in Table 2 and Figure 1.

COMPARISON OF SATELLITE, AUTO-TRAVERSE, AND MODEL TEMPERATURE PATTERNS

Satellite Temperature Patterns

Although much detail about the heat island of the study area is generated by the satellite data, only the main spatial features will be presented here, because comparison of the results of the three techniques (satellite, auto-traverse and modeling) is being emphasized. The three daytime HCMM-derived temperature patterns are shown in Figures 2 to 4. Several characteristics are common among the daytime temperature patterns. The central business district (CBD) is well defined in all three by an isotherm that conforms approximately to its shape. This region was among the warmest in the city on all three daytime temperature distributions. When the CBD temperatures are compared with the average temperatures of the coolest non-wet rural land cover, daytime heat islands of 5 to 6° C result. The smallest daytime heat island (approximately 5° C) corresponds to the only one of the three dates with measurable winds (2.0 m/sec). Also apparent on the three afternoon maps is a northward extension of high temperatures from the CBD along one of the major streets in the city; this represents, in addition to the CBD, the main commercial area in Gainesville. The November and December dates show a similar, although less distinct, eastward extension. The area of the University of Florida, to the west and southwest of the CBD, is manifested by the bending of isotherms around it, indicating that the many buildings and large parking lots there are conducive to higher temperatures.

Several other land-use-temperature relationships are distinguishable on the maps, such as the consistently high temperatures associated with the airport, in the extreme northeast portion of the city and with a large shopping mall located just outside the westernmost portion of the city limits, and the relatively uniform area of intermediate temperatures coincident with the largest contiguous zone of single-family housing in the city, located mostly to the northeast of the CBD. Consistently warm regions outside the urbanized area are characterized by bare ground/pasture land covers, which are most prevalent in a region six km east-northeast of the CBD and in the extreme southwest corner of the study area (see Figure 1). Rangeland in the southernmost portion of the study area is very warm on two of the daytime maps (Figures 3 and 4).

Another feature common to all three daytime temperature patterns is a stronger gradient to the immediate west of the CBD than to the east. This is probably partly the result of the commercial development to the east of the CBD and the riparian vegetation that occurs in sinuous segments to the west of the area.

The three satellite-derived temperature patterns obtained in the early morning (0230 LST) are shown in Figures 5 to 7. The 1 February 1979 pattern reveals fewer relationships between land cover and temperatures than the afternoon maps or the other two morning patterns. There are isolines of higher temperatures associated with the airport and the university campus, but generally there is very little temperature variation within the city or surrounding countryside. The urban heat island magnitude is only 1 to 2° C. Windspeed at the satellite overpass time was 4.0 m/sec, the greatest windspeed during any of the overpass times.

The other two early morning temperature patterns (Figures 6 and 7) show several definite correlations between land covers and temperatures. The 21 May 1978 map shows, like the afternoon maps, that an isoline very closely conforms to the CBD and university campus. These areas were the warmest in the city and exceeded representative rural temperatures by 4 to 6° C. Also similar to the afternoon patterns are higher temperatures extending northward and eastward from the CBD. The temperature pattern for the morning of 3 November 1978, shown in Figure 7, was acquired two days before the 5 November 1978 daytime pattern shown in Figure 3, and shows some similarities to that afternoon pattern and to the May morning pattern. Again, the isoline representing the highest temperature within the city is centered directly over the CBD, yielding a heat island of 9° C; the university campus is also warmer than its immediate surroundings. This maximum of 9° C corresponds closely to the 8.3° C value for a postsunset urban heat island predicted by Oke (1973) for a city the size of Gainesville. Narrow northward and eastward warm extensions stretch out from the CBD, and the temperature gradient is greater toward the western periperiphery of the city than toward the east.

Auto-Traverse Temperature Pattern

The auto-traverse data for this study were obtained from Dohrenwend and Wetterqvist (1977). An automobile-mounted Tele-thermometer, which can be read to 0.1° C, was used. The thermistor probe was shielded and mounted one metre above the roof of a light-colored auto to reduce radiational effects. The auto stopped to record each observation. A total of 63 temperature values were recorded over three transects through the city and into the undeveloped surroundings between 0455 and 0655 EST (before sunrise) on 9 December 1974. No time correction was applied to the data. Very light winds (less than 2.0 m/sec) and

Table 2. Land Use/Land Cover for Gainesville, Florida and Surrounding Area*

Category	Description for Gainesville Area
Residential: Single-family and Mobile Home	Predominantly 1 story units surrounded by vegetated surfaces
Residential: Multi-family	Mostly 1-4 story units; less vegetated than single-family
Commercial and Services	General commercial areas, including CBD and university campus; 1-3 stories dominate
Transportation, Communications, and Utilities	Main area is the airport in extreme northeast corner of city
Cropland and Pasture	Agricultural land, whether cultivated or fallow
Rangeland	Dry prairie, mostly located in Paynes Prairie, south of the city
Forest Land	Predominantly pine flatlands, commercial forests, and hardwood hammocks
Lakes	Largest is kidney-shaped Newnan's Lake on east side of study area
Forested Wetland	Cypress and hydric (wet) hammock
Nonforested Wetland	Marsh
Barren Land: Transitional areas	Generally land cleared for future commercial development

* Categories adapted from Anderson *et al.* (1976)

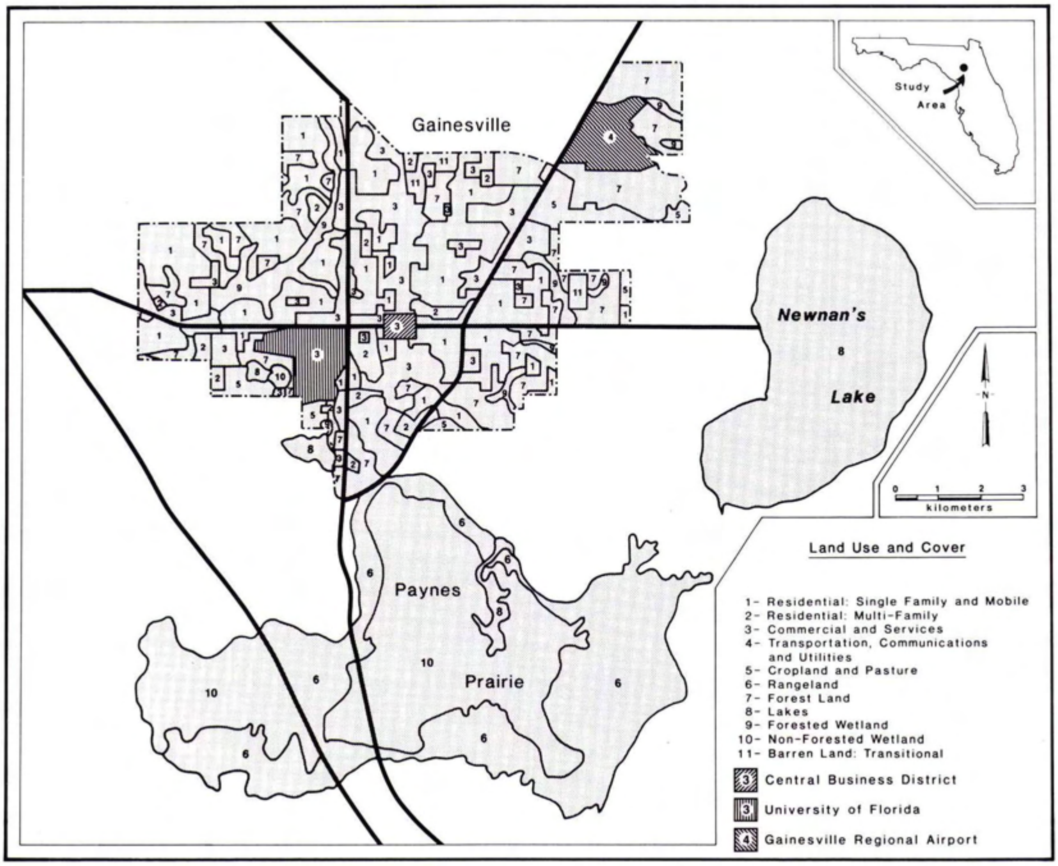

FIG. 1. Main physical features and land use/land cover.

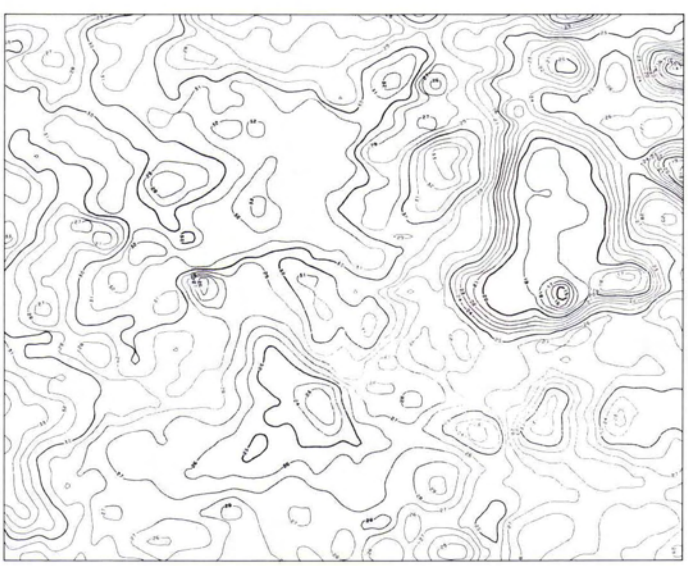

FIG. 2. HCMM-derived temperatures (°C) for 28 March 1979, 1330 LST.

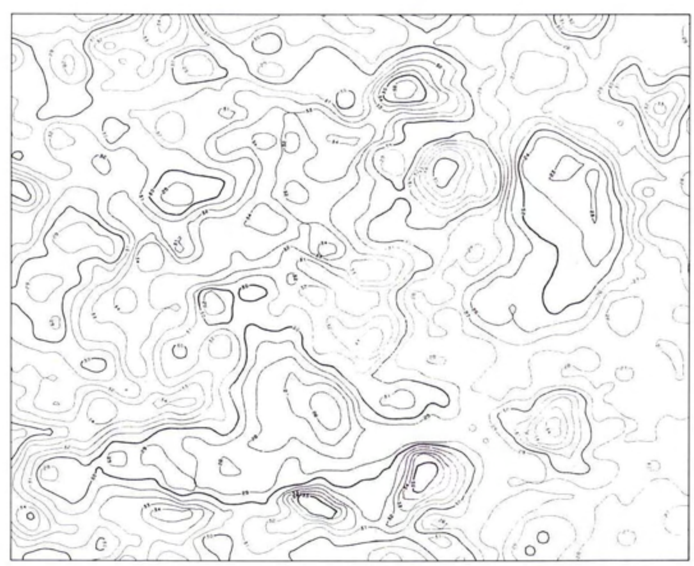

FIG. 3. As in Figure 2 except date is 5 November 1978.

calm conditions prevailed in the two-hour period. Only relative comparisons of isotherm patterns derived from the satellite and auto-traverse data can be made, because the former represent surface conditions and the latter represent conditions approximately two metres above the ground.

The temperature pattern resulting from the auto-traverse data is shown in Figure 8. Isotherms were determined from the data collection points by a computer graphics program. As with the satellite data, highest temperatures were recorded in and near the CBD. The highest temperature, 5.6° C, was recorded within the CBD; the two lowest temperatures, 2.6° and 3.2° C, were observed to the northwest and southeast, respectively, of the

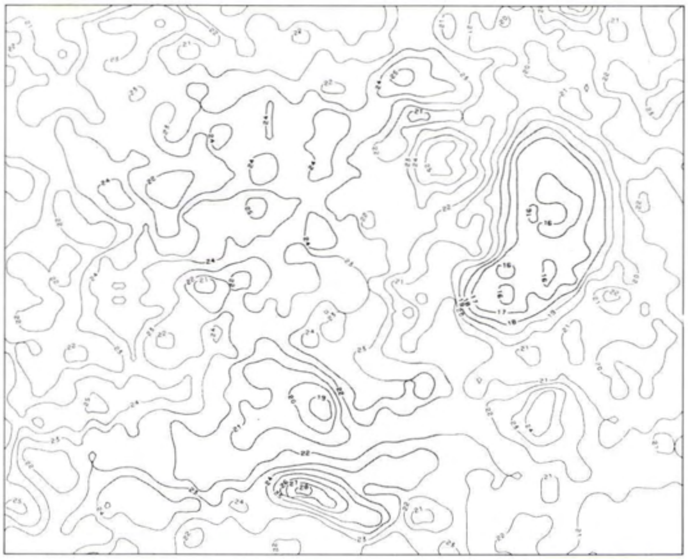

FIG. 4. As in Figure 2 except date is 17 December 1978.

FIG. 6. As in Figure 5 except date is 21 May 1978.

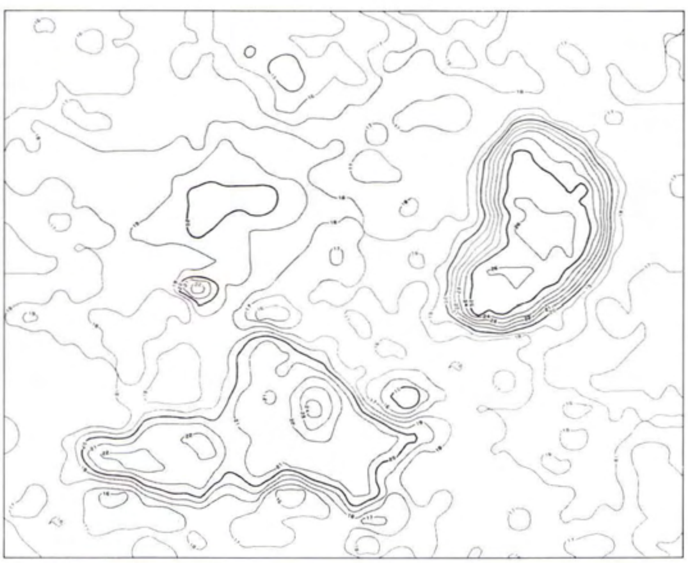

FIG. 5. As in Figure 2 except date/time is 1 February 1979, 0230 LST.

FIG. 7. As in Figure 5 except date is 3 November 1978.

city. The urban heat island magnitude was 3° C. High temperatures extended toward the north and east from the CBD, as was noted in the satellite temperature patterns. The auto-traverse pattern is closest in general resemblance to the satellite patterns of Figures 2 and 3. Also apparent was that the temperature gradient between the CBD and the urban periphery was stronger towards the western edge of the city than the eastern edge; this was also visible in most of the HCMM data. Although the auto-traverse temperatures were collected on only one date, and it is known that temperature patterns vary with seasons, meteorological conditions, and other factors, the findings basically agree with those of other urban heat island empirical results, and are generally similar to the HCMM-derived results.

COMPUTER-SIMULATED TEMPERATURE PATTERN

The model of Dohrenwend and Wetterqvist (1977) is a relatively simple land-use energy balance model. As noted by Todhunter (1986), this type of model assumes that differences between urban and rural temperatures are due to the unique radiative, thermal, and mechanical properties of the urban surface. The model used here is the DYNASPACE Meso Climate model, which is a component of a larger countywide land-use policy effect simulation model (Wetterqvist and Kaplan, 1976). The model simulates the temperature behavior of the atmosphere at shelter height as a function of land use. The model is not equivalent to state-of-the-art energy balance simulations. Rather, it is based on assigning land-use types to thermal categories based on various characteristics of the surface materials comprising the land uses. The model then produces a simple prediction of the temperature distribution that should theoretically occur.

Step one involved dividing the study area into 32-acre cells, resulting in 19,000 cells for our study area. A spectrum of ten thermal categories was designed, with the region of lowest diurnal and seasonal temperature variance and lowest maximum temperatures constituting one end of the spectrum (designated thermal category 1), and the region of highest diurnal and seasonal variance and highest maximum temperatures constituting the other end of the spectrum (thermal category 10). Exercising experienced judgement and employing published (e.g., Threlkeld, 1962; Sellers, 1965) values for the emissivity, heat capacity, albedo, aerodynamic roughness, and wet fraction (which is related to evapotranspiration) of the surface materials that occur in the study area, each of the 28 land-use types in the region was assigned to seven thermal categories, designated as thermal categories 2 to 8. Three other thermal categories (designated 1, 9, and 10) were reserved for additive thermal effects that occur when certain contiguous thermal regions exceed critical sizes. For example, when an area of thermal category 2 exceeded 20 cells, it was mapped as thermal category 1; if an area of thermal category 3 exceeded 100 cells, it was mapped as thermal category 1. In like fashion, a region of thermal category 6 was incremented to category 7 if the contiguous area was greater than 20 cells. Areas of category 7 and 8 were each incremented one category if the area exceeded 20 cells, and increased two categories if the area was greater than 100 cells. The DYNASPACE model then used these categories and the known distribution of the surface materials to output a map of *relative* temperature-behavior categories. As will be discussed below, the results closely coincide with post-sunset auto-traverse data.

The three-dimensional effects of the urban geometry are not directly considered in the model. That this exclusion may be a shortcoming of land-use energy balance models has been shown by Terjung and Louie (1974), Terjung and O'Rourke (1980), and Todhunter (1986). However, this problem is probably not as critical in Gainesville as in larger cities, because buildings taller than three stories are very rare, and only one is in the CBD. The major portion of the four-block-long CBD consists of buildings that are mostly only two stories in height.

The DYNASPACE model clearly predicts the existence of an urban heat island effect for Gainesville (Figure 9, using a simplified six-category scale). The main feature is the region of highest temperatures (category 6) that coincides very closely with the CBD, the university, and the northward extension of commercial land use from the CBD. The western boundary of this region of maximum urban heat island quite closely corresponds to the 4.5° C isotherm on the map obtained using the auto-traverse data (Figure 8). The only other region where the category-six thermal class occurs on the map of simulated temperature conditions is in the extreme northeastern portion of the city, coinciding with the airport. This warm region is also very conspicuous on all three daytime satellite maps. No auto-traverse temperatures were acquired in the vicinity of the airport. Also similar to the satellite-derived maps, and to the auto-traverse temperature pattern, are the northward and eastward extensions of the heat island effect, and a slightly greater thermal gradient to certain areas west of the area of predicted maximum urban effect, compared to the east.

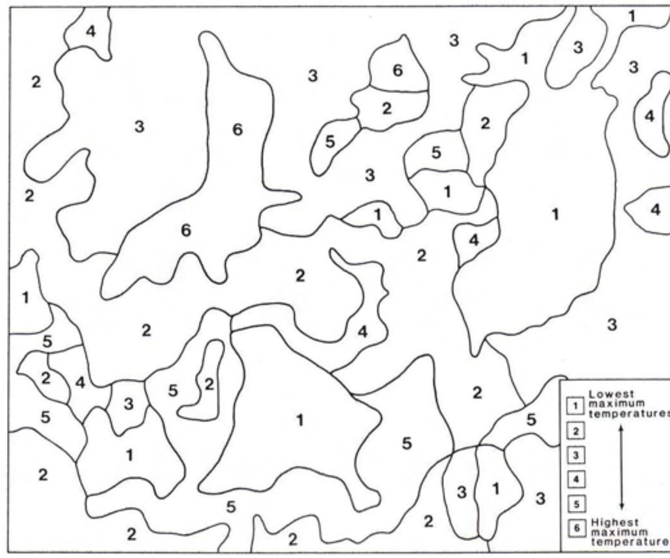

FIG. 9. Relative temperature-behavior categories predicted by the DYNASPACE model; derived from Dohrenwend and Wetterqvist (1977). Scale same as Figure 1.

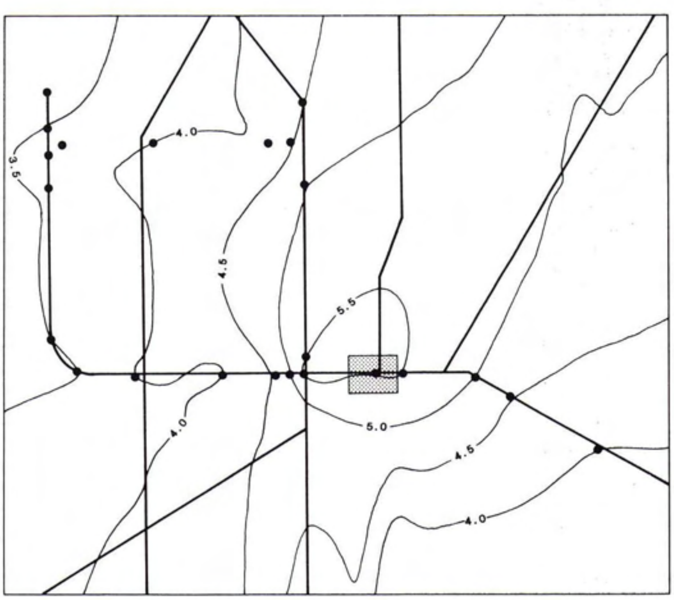

FIG. 8. Temperature pattern (°C) for 9 December 1974, 0455-0655 LST using the auto-traverse technique; derived from Dohrenwend and Wetterqvist (1977). Stippled area is CBD; scale is 1:75,000. Not all data collection points shown.

DISCUSSION

Although the three techniques produced generally similar spatial patterns of the basic aspects of the heat island, the absolute values of the heat island magnitudes varied widely between the satellite and auto-traverse techniques (the two of the three techniques for which absolute heat island magnitudes were determined). The satellite data revealed a heat island magnitude of a maximum of 9° C for the predawn data, whereas the value is 3° C based on the auto-traverse data. There are several potential reasons for these temperature differences. The data collection dates and times are different for the two techniques. The auto-traverse data were acquired in 1974 and the satellite data in 1978-79. However, because there was virtually no development or significant land-use/land-cover changes in the CBD (generally the warmest region in the auto-traverse and satellite data), the larger heat islands observed in the satellite data obtained 4 to 5 years after the ground data are not attributable to urban development. Seasonal variation is also probably not a primary contributing factor to the observed differences. The auto-traverse data were collected in December; the data of the postsunset satellite data with the greatest heat island was November. Additionally, meteorological conditions (particularly wind speed) were basically similar during times of the satellite and auto-traverse data, and winds were always less than 5.2 m/sec, which is the critical value for the elimination of the post-sunset heat island for a city the size of Gainesville predicted by the regression equation of Oke and Hannell (1970).

Probably the two reasons most responsible for the differences in the measured heat island magnitudes between the two techniques relate to the representative nature of the data. First, the satellite obtains a synoptic view, and is therefore able to measure all urban and rural thermal sources and sinks (within the resolution restriction of the sensor); the auto-traverse method has a much lower probability of including the areas that have the very highest and lowest temperatures in the urban-rural study area, or of producing temperature averages that are as representative of the general urban and rural land covers. Second, temperatures obtained by the auto-traverse technique basically represent shelter-height air temperatures, whereas the satellite-derived temperatures are representative of the radiatively-active surface. Geiger (1966) and Kalma *et al*. (1983) have noted temperature differences of 2.5 to 6.5° C between these surfaces during calm, clear conditions. Lenschow and Dutton (1964) reported summer differences of 9° C between ground and air temperatures. Goldreich (1985), however, found that, although ground and air temperature differed, the general thermal patterns of the urban heat island of Johannesburg obtained from an automobile-mounted thermometer and an aircraft-mounted thermal scanner were similar. The present study has shown this is also true when automobile-derived data are compared with satellite data, as well as with a model-simulated temperature pattern.

SUMMARY AND CONCLUSION

HCMM satellite thermal infrared digital data have been effectively used to show the spatial variation of the urban thermal patterns and several relationships between land use/land cover and satellite-derived temperatures in the relatively small city of Gainesville, Florida. Additional comparison studies could be undertaken using future satellite systems with finer resolution and overpass times close to those of HCMM. Welch (1982) has addressed sensor resolution requirements for urban studies. In relation to the present study, it can be seen that, although the 600-m resolution of the HCMM data is not sufficient for discerning relationships between temperatures and relatively small areas of a particular land use (e. g., an apartment complex), it is sufficient for providing a general characterization of intraurban temperature patterns. These patterns in Gainesville, Florida are generally consistent with those determined by ground-based observations and simulation modeling.

ACKNOWLEDGMENTS

This study was made possible by a joint study contract between the IBM Corporation, the University of Florida, and the Northeast Regional Data Center of the State University System of Florida. The authors are grateful to Dr. Virginia Hetrick of the Northeast Regional Data Center for assistance with the IBM 7350 Image Processing System, and to Mr. Doug Jordan of the Remote Sensing and Image Processing Laboratory within the Institute of Food and Agricultural Sciences at the University of Florida for his assistance with the ELAS image processing software. The authors also thank the reviewers for very constructive comments, and Dr. John Price for his atmospheric correction model and valuable criticism, and the National Space Science Data Center for the satellite data. Stephen Rogers performed all graphics.

REFERENCES

Anderson, J. R., E. E. Hardy, J. T. Roach and R. E. Witmer, 1976. *A Land Use and Land Cover Classification System for Use with Remote Sensor Data*, Geological Survey Professional Paper 964, U. S. Government Printing Office, Washington, D.C., 28 p.

Arnfield, A. J., 1982. An Approach to the Estimation of the Surface Radiative Properties and Radiation Budgets of Cities, *Physical Geography*, 3(2): 97–122.

Artis, D. A., and W. H. Carnahan, 1982. Survey of Emissivity Variability in Thermography of Urban Areas, *Remote Sensing of Environment*, 12(4): 313–329.

Auer, A. H., Jr., 1978. Correlation of Land Use and Cover with Meteorological Anomalies, *Journal of Applied Meteorology*, 17(5): 636–643.

Barnes, W. L., and J. C. Price, 1980. Calibration of a Satellite Infrared Radiometer, *Applied Optics*, 19(13): 2153–2161.

Brazel, A. J., and D. M. Johnson, 1980. Land Use Effects on Temperature and Humidity in the Salt River Valley, Arizona, *Journal of the Arizona-Nevada Academy of Science*, 15(2): 54–61.

Burt, J. E., P. A. O'Rourke, and W. H. Terjung, 1982. The Relative Influence of Urban Climates on Outdoor Human Energy Budgets and Skin Temperature I. Modeling Considerations, *International Journal of Biometeorology*, 26(1): 3–23.

Carlson, T. N., J. A. Augustine, and F. E. Boland, 1977. Potential Application of Satellite Temperature Measurements in the Analysis of Land Use over Urban Areas, *Bulletin of the American Meteorological Society*, 58(12): 1301–1303.

Carlson, T. N., J. K. Dodd, S. G. Benjamin, and J. N. Cooper, 1981. Satellite Estimation of the Surface Energy Balance, Moisture Availability and Thermal Inertia, *Journal of Applied Meteorology*, 20(1): 67–87.

Dohrenwend, R. E., and O. F. Wetterqvist, 1977. *Prediction of an Urban Heat Island from Land Use Patterns by Means of a DYNASPACE Model*, Urban and Regional Planning Series No. 8. Urban and Regional Planning Program, University of Florida, Gainesville, Florida.

Geiger, R., 1966. *The Climate Near the Ground*, third ed., Harvard University Press, New York, New York.

Goldreich, Y., 1985. The Structure of the Ground-Level Heat Island in a Central Business District, *Journal of Climate and Applied Meteorology*, 24(11): 1237–1244.

Goward, S. N., 1981. Thermal Behavior of Urban Landscapes and the Urban Heat Island, *Physical Geography*, 2(1): 19–33.

Hsu, S., 1984. Variation of an Urban Heat Island in Phoenix, *Professional Geographer*, 36(2): 196–200.

Kalma, J. D., G. F. Byrne, and M. E. Johnson, 1983. Frost Mapping in Southern Victoria: An Assessment of HCMM Thermal Imagery, *Journal of Climatology*, 3(1): 1–19.

Lenschow, D. H., and J. A. Dutton, 1964. Surface Temperature Variations Measured from an Airplane over Several Surface Types, *Journal of Applied Meteorology*, 3(1): 65–69.

Matson, M., E. P. McClain, D. F. McGinnis, Jr., and J. A. Pritchard, 1978. Satellite Detection of Urban Heat Islands, *Monthly Weather Review*, 106(12): 1725–1734.

Morgan, D., L. Myrup, D. Rogers, and R. Baskett, 1977. Microclimates Within an Urban Area, *Annals of the Association of American Geographers*, 67(1): 55–65.

National Aeronautics and Space Administration, 1980. *Heat Capacity Mapping Mission Users' Guide*, National Aeronautics and Space Administration, Goddard Space Flight Center, Greenbelt, Maryland, 120 p.

Nunez, M., and T. R. Oke, 1980. Modeling the Daytime Urban Surface Energy Balance, *Geographical Analysis*, 12(4): 373–386.

Oke, T. R., 1973. City Size and the Urban Heat Island, *Atmospheric Environment*, 7(8): 769–779.

———, 1982. The Energetic Basis of the Urban Heat Island, *Quarterly Journal of the Royal Meteorological Society*, 108(455): 1–24.

Oke, T. R., and F. G. Hannell, 1970. The Form of the Urban Heat Island in Hamilton, Canada, *Urban Climates*, WMO Technical Note No. 108, World Meteorological Organization, Geneva, pp. 113–126.

Outcalt, S. I., 1972. A Reconnaissance Experiment in Mapping and Modeling the Effect of Land Use on Urban Thermal Regimes, *Journal of Applied Meteorology*, 11(8): 1369–1373.

Pease, R. W., J. E. Lewis, and S. I. Outcalt, 1976. Urban Terrain Climatology and Remote Sensing, *Annals of the Association of American Geographers*, 66(4): 557–569.

Price, J. C., 1979. Assessment of the Urban Heat Island Effect Through the Use of Satellite Data, *Monthly Weather Review*, 107(11): 1554–1557.

———, 1983. Estimating Surface Temperature from Satellite Thermal

Infrared Data—A Simple Formulation for the Atmospheric Effect, *Remote Sensing of Environment*, 13(4): 353–361.

———, 1984. Comparison of the Information of Data from the Landsat 4 Thematic Mapper and the Multispectral Scanner, *IEEE Transactions on Geoscience and Remote Sensing*, GE-22(3): 272–281.

———, 1986. Remote Sensing in the Thermal Infrared, *Interpretation of Thermal Infrared Data: The Heat Capacity Mapping Mission*, edited by J.C. Price, Harwood Academic Publishers, London, pp. 187–196.

Rao, P. K., 1972. Remote Sensing of 'Urban Islands' from an Environmental Satellite, *Bulletin of the American Meteorological Society*, 53(7): 647–648.

Rayner, J. N., 1984. Simulation Models in Climatology, *Spatial Statistics and Models*, edited by G. L. Gaile and C. J. Willmott, D. Reidel Publishing, Dordrecht, Holland, pp. 417–442.

Sellers, W. D., 1965. *Physical Climatology*, University of Chicago Press, Chicago.

Taylor, S. E., 1979. Measured Emissivity of Soils in the Southeast United States, *Remote Sensing of Environment*, 8, 359–364.

Terjung, W. H., 1976. Climatology for Geographers, *Annals of the Association of American Geographers*, 66(2): 199–222.

Terjung, W. H., and S. S-F. Louie, 1973. Solar Radiation and Urban Heat Islands, *Annals of the Association of American Geographers*, 63(2): 181–207.

———, 1974. A Climatic Model of Urban Energy Budgets, *Geographical Analysis*, 6(4): 341–367.

Terjung, W. H., and P. A. O'Rourke, 1980. Simulating the Causal Elements of Urban Heat Islands, *Boundary-Layer Meteorology*, 19(1): 93–118.

Threlkeld, J. L., 1962. *Thermal Environmental Engineering*. Prentice-Hall International, London.

Todhunter, P. E., 1986. *A Comparison of Selected Surface Energy Balance Models in Urban Climatology*, Ph.D. dissertation, Department of Geography, University of California, Los Angeles.

Tuller, S. E., 1975. The Energy Budget of Man: Variations with Aspect in a Downtown Urban Environment, *International Journal of Biometeorology*, 19(1): 2–13.

Vukovich, F. M., 1983. An Analysis of the Ground Temperature and Reflectivity Pattern about St. Louis, Missouri, Using HCMM Satellite Data, *Journal of Climate and Applied Meteorology*, 22(4): 560–571.

———, 1984. A Comparison of Surface Temperature Derived from HCMM Infrared Measurements with Field Data, *Remote Sensing of Environment*, 15(1): 63–76.

Welch, R., 1982. Spatial Resolution Requirements for Urban Studies, *International Journal of Remote Sensing*, 3, 139–146.

Wetterqvist, O. F., and A. P. Kaplan, 1976. *Dynaspace Study, Gainesville/Alachua County, Florida—Development of a DYNASPACE Regional Land Policy Analysis System*, Technical Report, Departments of Architecture and Urban and Regional Planning, College of Architecture, University of Florida, Gainesville, Florida.

Winiger, M., 1982. *Topoclimatological Survey of Switzerland*, Final Report, HCMM Investigation HCM-021, Goddard Space Flight Center, Greenbelt, Maryland.

(Received 16 March 1988; revised and accepted 25 August 1988)

Forthcoming Articles

Steven G. Ackleson, AVHRR Observations of a Gulf of Maine Coccolithophore Bloom.
Michael H. Brill and *James R. Williamson*, Multi-Sensor DLT Intersection for SAR and Optical Images.
Christopher W. Brown, Daniel L. Civco, and *William C. Kennard*, Adaptation of a Hand-Held Radiometer for Measuring Upwelling Radiance in the Aquatic Environment.
Pat S. Chavez, Jr., Use of Variable Gain Settings on SPOT.
Pat S. Chavez, Jr., and *Andrew Yaw Kwarteng*, Extracting Spectral Contrast in Landsat Thematic Mapper Image Data Using Selective Principal Component Analysis.
Robert E Crippen, A Simple Spatial Filtering Routine for the Cosmetic Removal of Scan-Line Noise from Landsat TM P-Tape Imagery.
Mohamed Shawki Elghazali, Analytical Independent Model Triangulation Strip Adjustment Using Shore-Line Constraints.
Sabry F. El-Hakim, A Hierarchical Approach to Stereo Vision.
John G. Fryer and *Scott O. Mason*, Rapid Lens Calibration of a Video Camera.
Raymond J. Hintz, Christos Karakadas, and *Joon-Mook Kang*, Analysis of Pavement Cracking and Rutting Using Close-Range Photog raphy.
I.D. Kneppeck and *F.J. Ahern*, A Comparison of Images from a Pushbroom Scanner with Normal-Color Aerial Photographs for Detecting Scattered Recent Conifer Mortality.
V. Kratky., On-Line Aspects of Stereophotogrammetric Processing of SPOT Images.
Richard G. Lathrop, Jr., and *Thomas M. Lillesand*, Monitoring Water Quality and River Plume Transport in Green Bay, Lake Michigan with SPOT-1 Imagery.
Roop C. Malhotra, Potential of Large Format Camera Photography.
Larry R.G. Martin, Accuracy Assessment of Landsat-Based Visual Change Detection Methods Applied to the Rural-Urban Fringe.
Scott M. Rae, Two Non-Iterative Methods of Determining the Orientation of a Stellar Camera.
Urho A. Rauhala, Compiler Positioning System: An Array Algebra Formulation of Digital Photogrammetry.
Urho A. Rauhala, Don Davis, and *Ken Baker*, Automated DTM Validation and Progressive Sampling Algorithm of Finite Element Array Relaxation.
Donald C. Rundquist and *Liping Di*, Band-Moment Analysis of Imaging-Spectrometer Data.
J. Sneddon and *T.A. Lutze*, Close-Range Photogrammetric Measurement of Erosion in Coarse-Grained Soils.
James R. Williamson and *Michael H. Brill*, Dominant Geometry Combinations of Two- and Three-Point Perspective in Close-Range Applications.